Wire Array Z pinch precursors, implosions and stagnation

M.G. Haines, S.V.Lebedev, J.P.Chittenden, S.N. Bland, M. Sherlock, D.J. Ampleford, S.C. Bott, G.N. Hall, C. Jennings, J. Rapley
Blackett Laboratory, Plasma Physics Group, Imperial College, London SW7 2AZ

P.D. Le Pell, C.A. Coverdale, B. Jones and C. Deeney
Sandia National Laboratory, Albuquerque, NM

Abstract Recent measurements of the precursor ablation velocity show that the velocity is reduced significantly when the gap to core size ratio is less than π, implying a higher mass ablation rate and a change in the precursor density profile at the time of implosion. This might explain why experimentally there appears to be an optimal inter-wire gap for the shortest rise time of the x-ray pulse. 2-D kinetic modelling of the precursor plasma shows how long mean-free-path ions can lead to the accumulation of a central dense, radiating column. Precursor interaction with a foam cylinder is also modelled with material mixing allowed. Three effects are being studied that can increase the final x-ray radiation. One is the effect of later implosion of trailing mass, diagnosed by laser probing and modelled by 2-D simulations. A second mechanism is the development of m=1 instabilities and associated increase in ohmic dissipation from current path lengthening. The third is ion viscous heating arising from saturated non-linear, short wavelength MHD m=0 instabilities. Experimental evidence at 20MA on the Z-accelerator shows Doppler broadened spectra at stagnation with ion temperature in the 100-300 keV range, lending support for this last mechanism.

1. Introduction

The implosion dynamics of wire array z-pinches has been shown to be markedly different from that of a thin shell [1-5]. Essentially the current at first flows in the wires themselves which convert into a heterogeneous mixture of liquid and vapour, expanding radially at the vapour sound speed at the boiling point. The vapour around these wire cores breaks down and at this point carries most of the current. Erosion of the cores occurs through heat transfer from the surrounding plasma which is subjected to the global J × B force causing inward jetting. A simple rocket model relates the mass ablation rate, the J × B force and the resulting ablation velocity. The inward flowing precursor plasma has a regular axial structure attributed to an instability that could be electrothermal [6] (associated with the heat flux to the cores), Rayleigh-Taylor (associated with the acceleration) MHD (m = 0 mode) or some combination. The presence of the instability is instrumental in the later occurrence of gaps in the cores and the subsequent transfer of current to an inward moving piston that is snowplough-like in its dynamics [2, 4], and far more stable than an accelerated shell. On each side of the gaps in the cores material is left behind (the trailing mass), as is seen in laser probing images and gated x-ray emission, but can reconnect electrically at later times to give secondary implosions. At stagnation the rapid conversion of the kinetic energy of the implosion to give a high ion temperature and, by equipartition to electrons leads to intense X-ray radiation. However the energy radiated can sometimes be three to four times the kinetic energy [7-10]. Several mechanisms are explored in this paper.

2. Scaling of the Ablation Velocity

We have shown that the ablation velocity scales with the global magnetic field by employing conical wire arrays, and straight arrays of different diameters [11]. This is illustrated in Fig. 1.

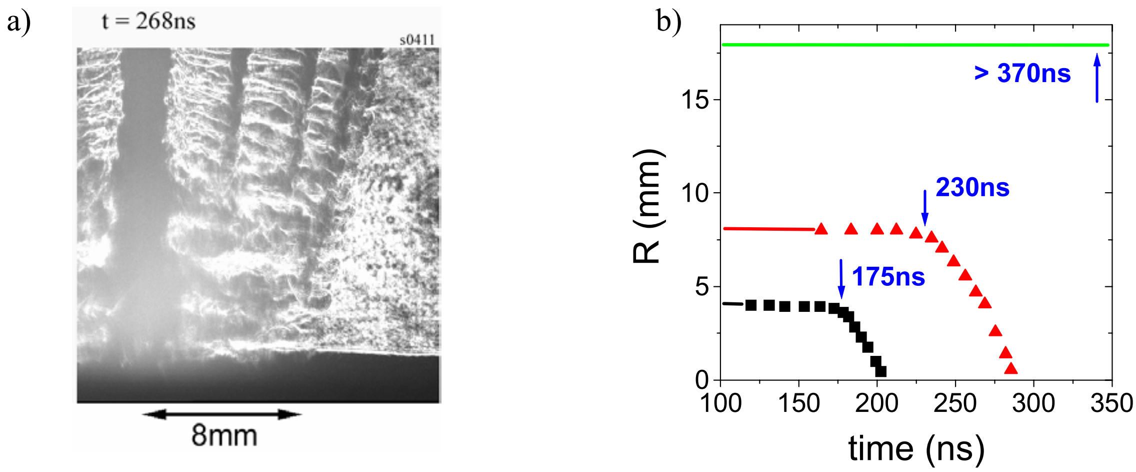

Fig. 1 Laser shadowgram of conical Al wire array (a) and implosion trajectories (b) measured from radial optical streaks for 32x15μm Al wire arrays of three different diameters.

In Fig. 1(a) the conical array shows clearly the effect of the higher global magnetic field at small radius where the wires are completely ablated at this time. In the straight arrays, Fig. 1(b) despite the same current per wire the implosion (at gap formation) occurs much earlier for the arrays of small diameter (8mm) compared to the 16mm and 36mm diameter arrays, which are each of 32 wires of 15μm Al. In addition it is found that there is a dependence of the ablation velocity on the ratio of the original gap between wires to the developed core size. The velocity is confirmed by end-on laser probing. For large gap/core size the ablation velocity approaches a constant value of typically 1.5×10^7 cm/s but reduces as shown in Fig.2 to about one third of this below a ratio of π which is the critical value where the global and private magnetic fields are equal.

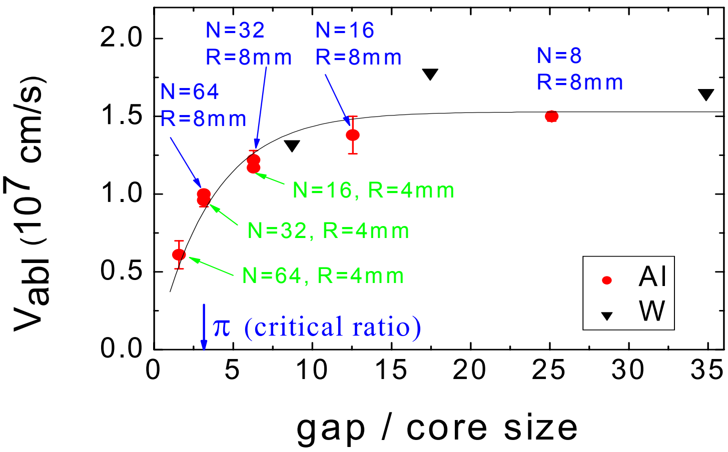

Fig. 2 Ablation velocity as a function of inter-wire separation for Al and W wire arrays. The inter-wire gaps are normalised on the core size measured by X-ray radiography. The line on the plot represents a fitting of the experimental data by a phenomenological formula $V_{abl} = 1.5x10^7(1- exp(-x/3.4)$, where V_{abl} is in cm/s and x=gap/core size.

The decrease in ablation velocity for small interwire separations could explain the existence of an optimal wire separation to give on stagnation the shortest rise time and largest peak power of the soft x-ray pulse, as found in recent Sandia experiments [4, 12].

The reduction in ablation velocity for small inter-wire gaps leads to a significant change in the radial density profile just prior to the main implosion, as the precursor plasma is closer to the wire array. This is shown in Fig.3 where the density profile is calculated for various values of the ablation velocity.

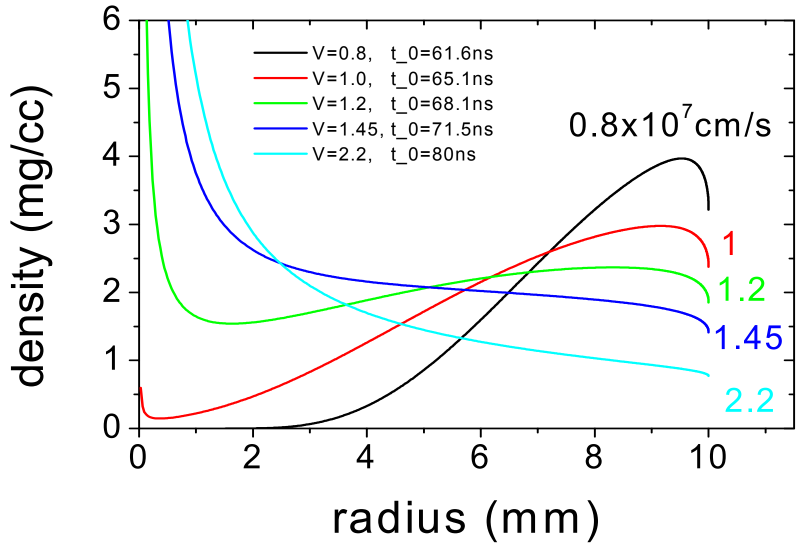

Fig. 3. Density profiles along the implosion trajectories, calculated for different values of the ablation velocities.

Thus this case will behave in a more shell-like way, and could be subject to the Rayleigh-Taylor instability.

3. Simulation of the Precursor Plasma

Finite ion-ion mean-free-path effects in the precursor plasma have been modelled with a hybrid model which provides a kinetic description of the ion interactions [13]. In tungsten the streaming precursor plasma heads toward the axis and initially interpenetrates giving rise to an axially-peaked density profile. The density of the streams and thus the density of the plasma on-axis increases with time until the system becomes collisional. This results in a non-linear drop in the ion temperature in the denser regions which in turn gives rise to the rapid formation (within $\leq 10ns$) of a highly compact radiating plasma on the axis. This effect is shown in Fig.4(a) in two dimensions.

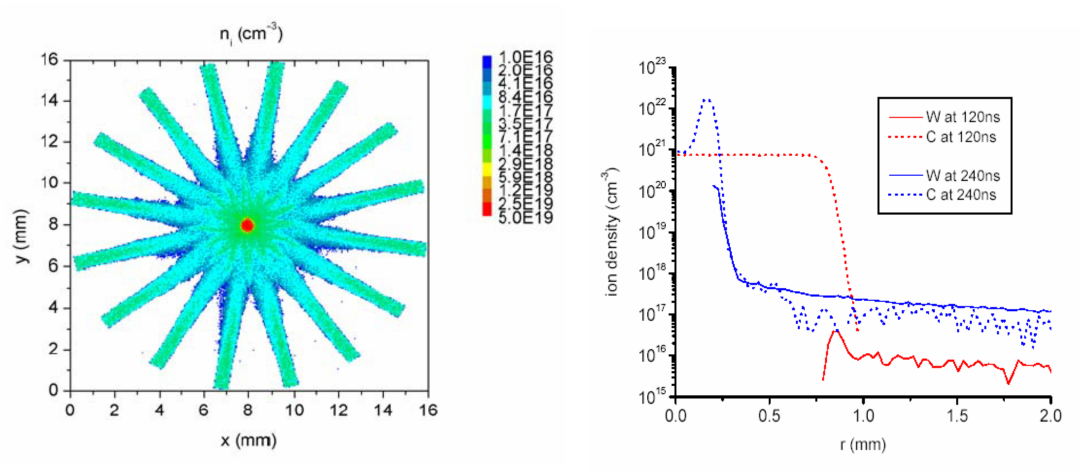

(a) (b)

Fig. 4(a) The W ion density in the precursor plasma at 230ns and (b) the W and C ion densities at two different times during the interaction between the precursor streams (W) and a foam target (C).

The model has also been used to study the interaction between W precursor streams and a cylindrical foam target placed on axis. The target was approximated by a cold, solid-density Carbon plasma. With conditions relevant to MAGPIE, it was found that the streams ablate the outer surface of the plasma giving rise to collisionless flow of high energy C ions against the incoming W flow. At later times, when the streams are more dense, they are capable of compressing the target, as shown in Fig4(b). This could have important implications for the dynamic hohlraum concept.

4. 3-D MHD Simulations

2-D and 3-D MHD simulations of the effect of the inward flowing streamers, the subsequent implosion confirm the experimental evidence of trailing mass. With a pragmatic choice of resistivity, current reconnection can occur with secondary implosions that affect the x-ray pulse. Figure 5 shows 3-D simulations of these effects for MAGPIE conditions, with a 16mm diameter array of 15 μm diameter aluminium wires driven by currents that rise to 1.5 MA in about 200ns. The wires are initiated with an axial temperature perturbation. Low density coronal plasma is accelerated towards the axis to form a dense precursor column, the fraction of current in which is small; some experiments suggest negligible. The simulations [14] here show the final implosion commencing at 200ns and peak compression at 243ns with trailing mass carrying about half the current which arrives on axis later. In this simulation the heating by m=1 activity accounts for 30% of the X-ray yield.

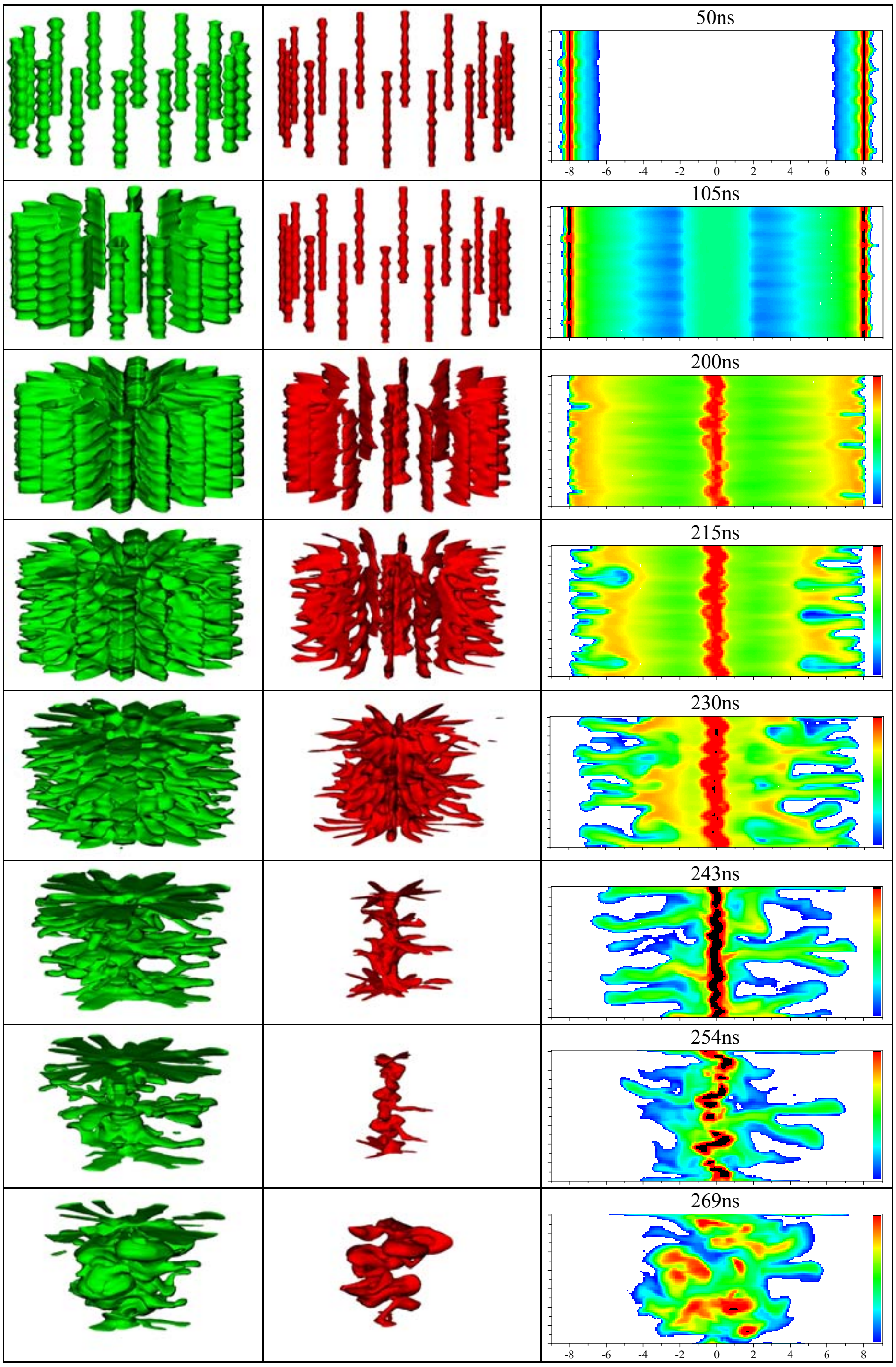

Figure 5. Surfaces of constant density for 0.003 kg/m^3 (green) and 0.1 kg/m^3 (red), and contours of the logarithm of mass density, in a slice through the x-z plane.

5. m=0 MHD Instabilities and Ion Viscous Heating

A new mechanism has been proposed to explain the significantly larger energy that is radiated at stagnation compared to the kinetic energy of the initial implosion. This is based on the development of fast growing short wavelength (of order the ion Larmor radius) m=0 interchange MHD modes, their saturation and the accompanying ion viscous heating. A viscous Lundqvist number of 2 is assumed to determine the wavelength of the fastest growing mode. The nonlinear saturation of the mode will occur when the second order convective term in the equation of motion equals the linear acceleration term. Then the eddy velocity amplitude will be smaller than the Alfven speed by a factor $\sqrt{(ka)}$ where k is the perturbation wave number and a is the pinch radius, ka being of order 10^3. The perturbed magnetic field fluctuation is $(ka)^{-1}$, even smaller. Nevertheless the viscous heating rate is on the nanosecond timescale in the 20MA Z-experiments at Sandia. Equating this heating to the equipartition rate to the electrons leads to ion temperatures in the 100 to 300 keV range in conditions relevant to experiments on Z at Sandia.

Recent spectroscopic data on the Z-accelerator confirms such high ion temperatures in stainless steel arrays. The viscous heating is particularly effective for interchange modes because part of the viscous heating is from terms that are not reduced by ion magnetisation.

References

[1] LEBEDEV S.V. et al 2000, Phys. Rev. Lett. 85, 98
[2] LEBEDEV S.V. et al 2001, Phys. Plasmas 8, 3734
[3] ALEKSANDROV V. V. et al 2001, Plasma Phys. Rep. 27, 89
[4] LEBEDEV S.V. et al 2002, Phys. Plasma 9, 2293
[5] BEKHTEV M.B. et al 1989, Sov. Phys. – JETP 68, 955
[6] HAINES M.G. 1981, Phys. Rev. Lett. 47, 917
[7] DEENEY C. et al 1997, Phys. Rev. E 56, 5945
[8] DEENEY C. et all 1999, Phys. Plasma 6, 3576
[9] APRUZESE J.P. et al 2001, Phys. Plasmas 8, 3799
[10] COVERDALE C.A. et al 2002, Phys. Rev. Lett. 88, 065001
[11] LEBEDEV S.V. et al, Nucl. Fusion *to be published*
[12] MAZARALEIS M. et al, 2002 Bull. Am. Phys. Soc. 67, 4313
[13] SHERLOCK M. et al 2004, Phys. Plasma 11, 1609
[14] CHITTENDEN J.P. et al Plasma Phys. Control Fusion *to be published*